ACS Chemical Neuroscience

Research Article

pubs.acs.org/chemneuro

Cytotoxicity of Mutant Huntingtin Fragment in Yeast Can Be Modulated by the Expression Level of Wild Type Huntingtin Fragment

Aliabbas Ahmedbhai Saleh, Ankan Kumar Bhadra, and Ipsita Roy*

Department of Biotechnology, National Institute of Pharmaceutical Education and Research (NIPER), Sector 67, S.A.S. Nagar, Punjab 160 062, India

Supporting Information

ABSTRACT: Conflicting reports exist in the literature regarding the role of wild-type huntingtin in determining the toxicity of the aggregated, mutant huntingtin in Huntington's disease (HD). Some studies report the amelioration of toxicity of the mutant protein in the presence of the wild-type protein, while others indicate sequestration of the wild-type protein by mutant huntingtin. Over the years, yeast has been established as a valid model organism to study molecular changes associated with HD, especially at the protein level. We have used an inducible system to express human huntingtin fragments harboring normal (25Q) and pathogenic (103Q) polyglutamine lengths under the control of a galactose promoter in a yeast model of HD. We show that the relative expression level of each allele (wild-type/mutant) decides the cellular phenotype. When the expression level of wild-type huntingtin is high, an increase in the solubility of the mutant protein is observed. Fluorescence-recovery-after-photobleaching (FRAP) studies show that solubility reaches ~94% in these cells. This leads to reduction in oxidative stress and cytotoxicity, and increases cell viability. In-cell FRET studies show that interaction between these proteins does not require the presence of a mediator. When the expression of wild-type huntingtin is low, it is sequestered into aggregates by the mutant protein. Even under these conditions, cytotoxicity is attenuated. Our findings indicate that the presence of wild-type huntingtin has a beneficial role even when its relative expression level is lower than that of the mutant protein.

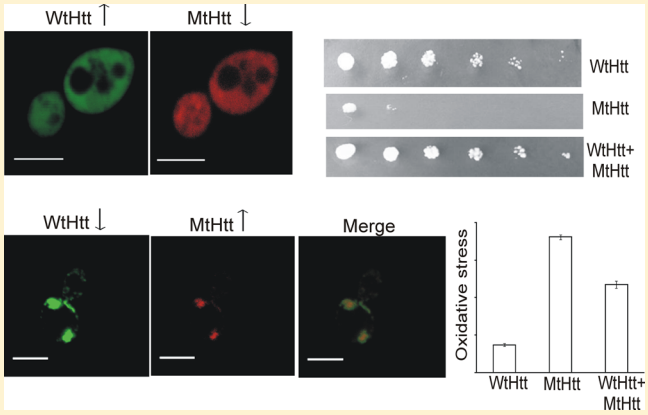

KEYWORDS: *Chaperone, gene dosage, huntingtin, Huntington's disease, protein misfolding*

Huntington's disease (HD) is a devastating progressive neurodegenerative disorder which is characterized by motor impairment, personality change, chorea (involuntary movements), and psychiatric symptoms. The formation of cytoplasmic or neuronal inclusions is a hallmark of the disease.[1,2] The major constituent of these inclusions is a protein called huntingtin (htt), with an elongated polyglutamine (polyQ) tract at its N-terminus.[3] The length of the polyQ stretch in the wild type protein ranges from 6 to 36. If the length exceeds 39, the mutant protein starts to aggregate, resulting in neurodegeneration. The extent of aggregation has been positively correlated with cytotoxicity.[1,2,4] Inhibition of aggregation of mutant huntingtin is thus a promising strategy to slow down the progress of the disease.

The function of the wild type protein is not completely clear. It has been suggested to have an antiapoptotic role; it offers protection to conditionally immortalized striatal cells against apoptosis-stimulatory conditions such as serum deprivation and exposure to 3-nitropropionic acid, a mitochondrial Complex I inhibitor.[5] It is important in vesicular trafficking of brain-derived neurotrophic factor (BDNF) via HAP-1.[6] The role of wild type huntingtin in embryonic development is again ambiguous. *Htt*-null mice die before gastrulation.[7] However, patients homozygous with pathogenic polyQ length do not exhibit any anomaly during birth.[8] This suggests that while the protein is essential for embryogenesis, the length of the polyQ tract is not important during development.

The mechanism of disease progression and the role of wild type and mutant alleles in the process are debatable. The expansion of polyQ stretch has been suggested to confer the mutant protein with a toxic gain of function. Evidence for this comes from reports of formation of SDS-resistant fibrillar aggregates by a nucleation-dependent route.[1,9] These aggregates have been shown to sequester the wild type protein,[10] thus hinting at the possibility of loss of function as a cause of the disease. They also sequester other polyQ-containing proteins, mainly transcription factors like TATA-binding

Received: September 19, 2013
Revised: December 26, 2013
Published: December 30, 2013

protein (TBP), CREB-binding protein (CBP), and so forth,[11] which supports the premise of the polar zipper model.[12] Thus, the interaction between wild type and mutant huntingtin assumes importance. The length of the polyQ tract in the mutant protein is directly proportional to the severity of symptoms and shows an inverse correlation with the age of onset of HD.[13,14] A longer length in the wild type protein is associated with delayed onset of the disease in patients with a longer polyQ tract in the mutant protein.[13,15] Longer length of the polyQ tract in the wild type protein coupled with shorter polyQ length in the mutant protein is associated with an earlier onset of the disease.[16] This is linked to the appearance of more severe symptoms and faster neuronal atrophy.

Conflicting studies have been reported in the literature regarding interaction between wild type and mutant huntingtin. The presence of mutant huntingtin N-terminal fragment (52Q) led to the formation of SDS-insoluble fibrillar coaggregates with normal length huntingtin (20Q or 32Q).[10] The amount of aggregates correlated with the total length of polyQ tract, irrespective of whether it exceeded the critical polyQ length. On the other hand, wild type huntingtin has been reported to reduce toxicity due to mutant huntingtin (72Q) in neuronal as well as non-neuronal cell lines.[17] The cause of this beneficial effect was not reported; it was not due to decreased protein aggregation as inclusions were present even as cytotoxicity was reduced. YAC72 mice [expressing human huntingtin with 72Q, in the absence of endogenous mouse huntingtin (*Hdh*−/−)] required a higher level of wild type mouse *huntingtin* (+/+, i.e. 100% of normal endogenous *huntingtin* level) to rescue testicular degeneration than YAC46 mice (which required ±, i.e. 50% of normal endogenous *huntingtin* level).[18] Again, the cause of the positive response due to the presence of the wild type protein was not discussed. These studies suggest that the interaction between wild type and mutant length huntingtin does influence the phenotype of the cells expressing these proteins. What is not clear is the cause of such behavior and the variation in response observed in different cases. In this work, we explore how the expression of wild type huntingtin influences the propensity of the mutant protein to aggregate and vice versa. We show that the differential behavior observed is due to the dosage of the respective allele and that by modulating the copy number of each gene, the phenotype of cells harboring them can be predicted.

RESULTS AND DISCUSSION

Coexpression with Wild Type Protein Increases Solubility of Mutant Huntingtin. When expressed alone, 25Q-htt-EGFP was expressed as a soluble protein while 103Q-htt-mRFP was observed as fluorescent puncta (Figure 1A), indicating formation of aggregates. When coexpressed with 25Q-htt-EGFP, 103Q-htt-mRFP (from pRS315-*103Q-htt-mRFP*, Figure S1, Supporting Information) was expressed in the soluble form (Figure 1A). Native PAGE analysis of cell lysates coexpressing 25Q-htt-EGFP and 103Q-htt-mRFP showed that the expression of 25Q-htt-EGFP was not affected in the presence of 103Q-htt-mRFP (Figure 1B). No band for soluble monomeric 103Q-htt-mRFP could be seen in cells expressing the mutant protein alone while a band for the monomeric protein was seen in cells coexpressing wild type and mutant proteins (Figure 1B). Thus, in the presence of 25Q-htt-EGFP, 103Q-htt-mRFP was partitioned off into the soluble fraction. This was also confirmed by immunoblotting with FLAG (Figure 1C) and polyQ (Figure 1D) antibodies. The

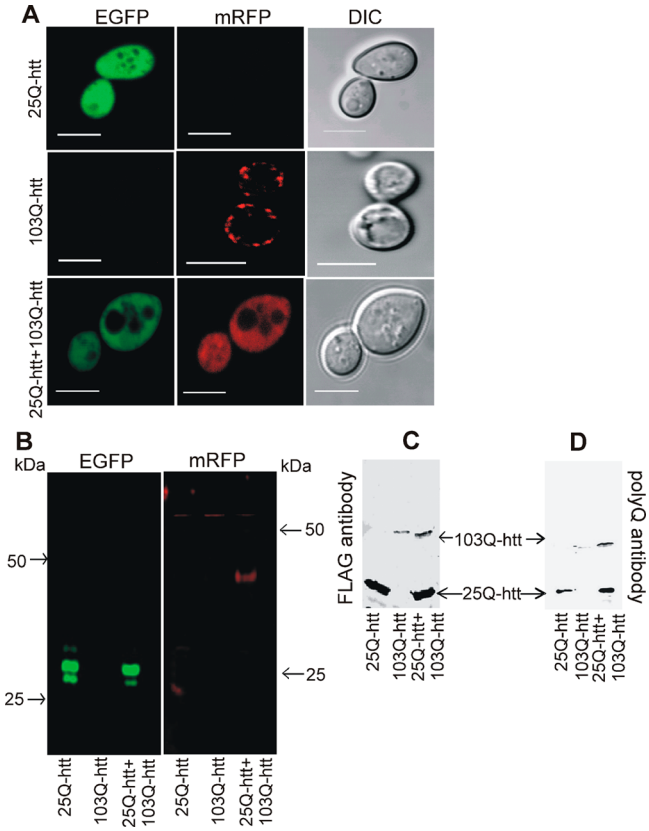

Figure 1. Coexpression of 25Q-htt and 103Q-htt leads to the solubilization of the latter. (A) Confocal microscopy of cells expressing 25Q-htt-EGFP (excitation at 488 nm and emission at 510 nm) and 103Q-htt-mRFP (excitation at 547 nm and emission at LP 650 nm) alone and together. Cells were visualized under 100× objective. Bar = 10 μm. (B) Native PAGE (12% cross-linked polyacrylamide gel) analysis of cell lysates expressing 25Q-htt-EGFP and 103Q-htt-mRFP. Gel was scanned in GFP and RFP modes on an image scanner (Typhoon Trio, GE Healthcare, Sweden). Molecular weight markers indicate positions of standard proteins on the same gel stained with Coomassie Blue. (C) Western blotting of cell lysates expressing 25Q-htt-EGFP and 103Q-htt-mRFP. The membrane was probed with mouse FLAG antibody (1:1000) as the primary antibody. For densitometric analysis, the intensity of the band for 25Q-htt-EGFP or 103Q-htt-mRFP when expressed alone was assigned an arbitrary value of 1 and the corresponding band intensities of 25Q-htt-EGFP or 103Q-htt-mRFP in coexpressing cells was calculated taking this as the base value. (D) Western blotting of cell lysates expressing 25Q-htt-EGFP and 103Q-htt-mRFP. The membrane was probed with mouse polyQ antibody (1:5000) as the primary antibody.

expression level of 25Q-htt-EGFP remained largely unaltered in singly expressing or coexpressing cells. The band intensity of the monomeric 103Q-htt-mRFP protein, however, increased significantly when coexpressed with 25Q-htt-EGFP when detected with either FLAG or polyQ antibody. Densitometric analysis of the immunoblot probed with FLAG antibody showed 2.7-fold increase in the intensity of the band for 103Q-htt-mRFP in coexpressing cells as compared to the cells expressing the mutant protein alone.

Yeast cells were monitored for the solubilization of 103Q-htt-mRFP by fluorescence recovery after photobleaching (FRAP). For this, cells expressing 103Q-htt-mRFP alone or along with 25Q-htt-EGFP were observed under a confocal scanning laser microscope (Eclipse, model E600, Nikon Corporation, Japan). The recovery after photobleaching was much less in case of

dx.doi.org/10.1021/cn400171d | *ACS Chem. Neurosci.* 2014, 5, 205−215

103Q-htt-mRFP expressed alone and in the aggregated form as compared to 103Q-htt-mRFP expressed in the soluble form in the presence of 25Q-htt-EGFP (Figure 2). The mobile fraction

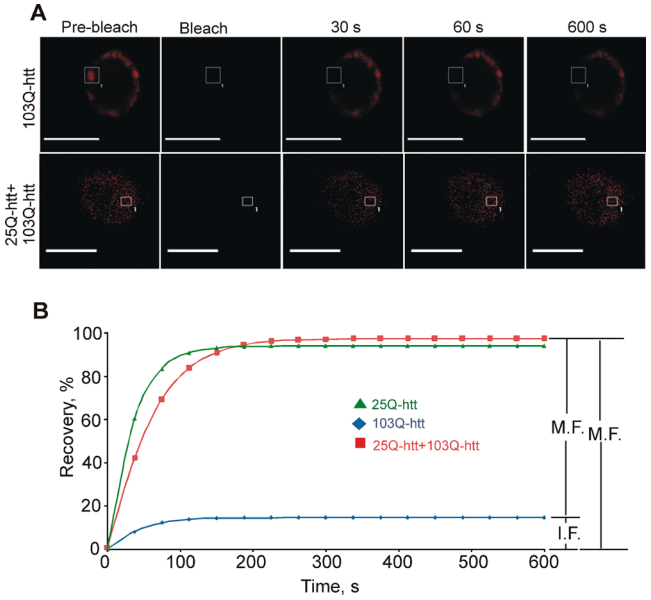

Figure 2. FRAP analysis. (A) Photobleaching and subsequent recovery in a cell expressing 103Q-htt-mRFP alone and along with 25Q-htt-EGFP. Region of interest is shown by a white square. Images for a single cell are shown. (B) Recovery curve of 103Q-htt-mRFP after photobleaching. Recovery after photobleaching of htt-25Q-EGFP is shown for comparison. M.F.: mobile fraction; I.F.: immobile fraction.

was calculated to be less than 13.1 ± 3.8% (mean ± s.e.m.) and approximately 92.7 ± 4.9% when 103Q-htt-mRFP was expressed alone and in the presence of 25Q-htt-EGFP, respectively (Figure 2). For comparison, the mobile fraction of 25Q-htt-EGFP was calculated to be 95.3 ± 3.4%. This confirms the solubilization of 103Q-htt-mRFP in the presence of 25Q-htt-EGFP. Aggregated 103Q-htt-mRFP is less mobile in nature and remains localized in particular areas of the cell while in the presence of the wild type protein, soluble 103Q-htt-mRFP is highly mobile, its solubility being of a similar level as that of the wild type protein. Transcriptional activation of endogenous Drosophila huntingtin by Engrailed shows a protective role in the aggregation of mutant human huntingtin.[19] The level of solubilization is lower in this case than that observed by us although the difference is not significant.

Coexpression of Wild Type and Mutant Huntingtin Reduces Stress and Toxicity in Yeast Cells. Aggregation of misfolded huntingtin has been linked to increased level of reactive oxygen species (ROS), resulting in cellular toxicity in yeast.[20] Solubilization of 103Q-htt-mRFP should lead to attenuation of oxidative stress and relieve toxic insult to cells. When expressed alone, 103Q-htt-mRFP was present as aggregates (Figure 1A). The level of ROS in these cells was significantly higher as compared to yeast cells expressing 25Q-htt-EGFP alone (Figure 3A). When coexpressed with 25Q-htt-EGFP, the level of oxidative stress, measured by the fluorescence intensity of dichlorofluorescein (de-esterified and oxidized metabolite of DCFH-DA), decreased significantly (Figure 3A), signifying reduction in the level of ROS generated in cells expressing 103Q-htt-mRFP in the soluble form.

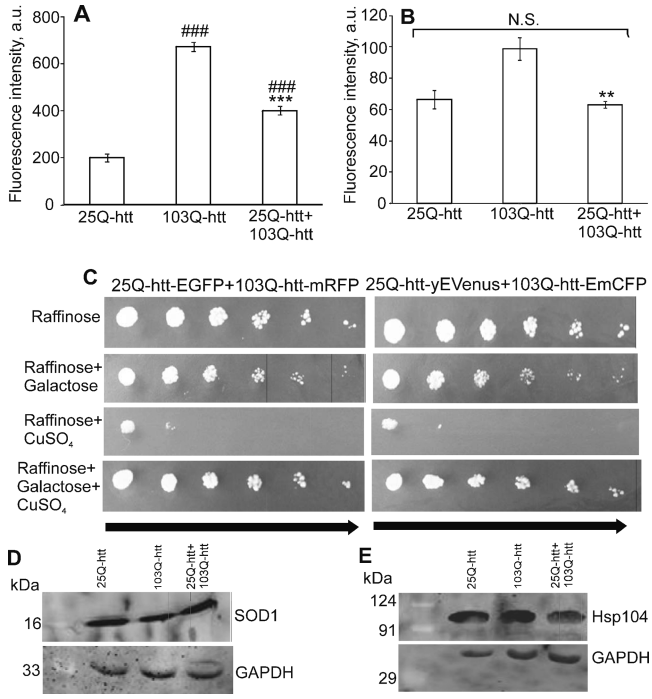

Figure 3. Toxicity in yeast cells expressing 103Q-htt. (A) Oxidative stress in yeast cells expressing 103Q-htt alone and along with 25Q-htt was measured by DCFH-DA assay. (B) Cytotoxicity was measured in cells expressing 103Q-htt alone and along with 25Q-htt by Sytox orange. Values shown are mean ± SEM of three independent experiments. $^{**}p < 0.01$, $^{***}p < 0.001$ against cells expressing 103Q-htt alone; $^{###}p < 0.001$ against cells expressing 25Q-htt alone. (C) Cell viability assay was carried out by serially diluted cells (starting with 9×10^3 cells, diluted 3-fold) transformed with *25Q-htt-EGFP/103Q-htt-mRFP* or *25Q-htt-yEVenus/103Q-htt-EmCFP* as indicated on selection plates. Arrow indicates direction of dilution. Growth was monitored at 30 °C for 2−3 days. (D) Western blotting of cell lysates expressing 25Q-htt-EGFP and 103Q-htt-mRFP. The membrane was probed with rabbit SOD1 antibody (1:1000) as the primary antibody and antirabbit FITC-conjugated antibody (1:1000) as the secondary antibody. The expression of GAPDH was used as the loading control and was monitored using GAPDH antibody (1:2000) as the primary antibody and antimouse FITC-conjugated antibody (1:2000) as the secondary antibody. (E) Western blotting of cell lysates expressing 25Q-htt-EGFP and 103Q-htt-mRFP. The membrane was probed with rabbit Hsp104 antibody (1:100 000) as the primary antibody and antirabbit FITC-conjugated antibody (1:1000) as the secondary antibody. The expression of GAPDH was used as the loading control and was monitored using GAPDH antibody (1:2000) as the primary antibody and antimouse FITC-conjugated antibody (1:2000) as the secondary antibody. For densitometric analysis, the ratio of intensities of the band for SOD1 or Hsp104 to the band for the loading control (GAPDH) in cells expressing 25Q-htt-EGFP alone was assigned an arbitrary value of 1 and other values were calculated taking this as the base value.

Damage to plasma membrane due to expression of 103Q-htt-mRFP was measured using Sytox orange. Sytox orange is a high-affinity nucleic acid stain that penetrates cells with compromised plasma membranes but not live cells with intact plasma membranes.[21] When 103Q-htt-mRFP was expressed alone as aggregates, the cytotoxicity was higher as compared to cells expressing 25Q-htt-EGFP alone (Figure 3B). In cells coexpressing 25Q-htt-EGFP and 103Q-htt-mRFP, cytotoxicity was reduced significantly and was similar to the level of fluorescence intensity of cells expressing 25Q-htt-EGFP alone

dx.doi.org/10.1021/cn400171d | ACS Chem. Neurosci. 2014, 5, 205−215

(Figure 3B). Since aggregated mutant huntingtin has been correlated with increased oxidative stress and toxicity in cells,[20] these results confirm the beneficial effect of the coexpression of 25Q-htt-EGFP with 103Q-htt-mRFP in these cells.

The viability of yeast cells expressing 25Q-htt and/or 103Q-htt was checked by plating the cells on different media, which would selectively express one or both proteins. When yeast cells cotransformed with pYES2-*25Q-htt*-EGFP and pRS315-*103Q-htt-mRFP* were plated on raffinose alone (neither protein was expressed), maximum growth was seen (Figure 3C). On induction of expression of 25Q-htt-EGFP with 2% galactose (to induce *GAL1* promoter), the cell viability decreased marginally. When cells were induced with 500 μM $CuSO_4$ (to induce *CUP1* promoter), 103Q-htt-mRFP was expressed in the aggregated fraction. Cells which expressed 103Q-htt alone showed significantly reduced viability as compared to cells expressing 25Q-htt-EGFP or no huntingtin (Figure 3C). This correlated with higher oxidative stress and enhanced permeability of cell membrane in these cells. When expression of 25Q-htt was coinduced along with that of 103Q-htt and mutant huntingtin was expressed in the soluble form, this loss of viability was rescued (Figure 3C). Thus, when oxidative stress was reduced and cell membrane permeability was not compromised, the cells grew to the same level as those expressing 25Q-htt alone (Figure 3C). In order to confirm if this observed beneficial effect of the expression of 25Q-htt was in any way due to the tags fused to the proteins, we decided to change the fluorescent tags of 25Q-htt and 103Q-htt. The wild type protein was expressed as a fusion protein with yEVenus (25Q-htt-yEVenus, from pYES2-*25Q-htt-yVenus*), while the mutant protein was expressed as a fusion protein with EmCFP (103Q-htt-EmCFP, from pRS315-*103Q-htt-EmCFP*) (Figure S2, Supporting Information). When expression was induced with 2% galactose, 25Q-htt-yEVenus was expressed in the soluble form (Figure 4A). When induced with 500 μM $CuSO_4$, 103Q-htt-EmCFP was seen to be expressed as fluorescent puncta, confirming that the mutant protein was present in the aggregated form (Figure 4A). On being coexpressed with 25Q-htt-yEVenus, 103Q-htt-EmCFP was expressed in the soluble form (Figure 4A). This confirmed that the solubilization of 103Q-htt in the presence of 25Q-htt was independent of the fluorescence tag employed. The pattern of cell viability observed was also the same as that seen with the earlier pair of proteins (Figure 3C). The uninduced cells showed the maximum growth on raffinose. Viability was marginally affected when cells expressed 25Q-htt-yEVenus and significantly affected when cells were induced to express 103Q-htt-EmCFP alone. In the presence of 25Q-htt-yEVenus, however, toxicity due to 103Q-htt-EmCFP was reduced (Figure 3C), confirming the advantage associated with the presence of the wild type protein.

Interaction Analysis between Wild Type and Mutant Huntingtin. In-cell FRET can be a useful tool to study the interaction between two protein molecules fused to fluorophores of the appropriate absorption and emission spectra. 25Q-htt-yEVenus and 103Q-htt-EmCFP were coexpressed in yeast cells and observed under a confocal laser scanning microscope (Eclipse, model E600, Nikon Corporation, Japan) (Figure 4A). The acceptor fluorophore, 25Q-htt-yEVenus, was photobleached and the fluorescence intensity of 103Q-htt-EmCFP was measured before and after photobleaching. Maximum $FRET_{eff}$[22] was calculated to be 30.2% (D_{pre} = 970.3 and D_{post} = 1391.0) and the range of $FRET_{eff}$ was 25.6 ± 5.1% (mean ± SEM). The scanning micrographs showed increased fluorescence intensity of 103Q-htt-EmCFP after photobleaching (Figure 4B). Increase in FRET efficiency by up to 25% suggests strong interaction between the fluorescently tagged proteins,[22] that is, wild type and mutant huntingtin in this case. This direct interface also suggests the redundancy of any other cellular protein in mediating this interaction.

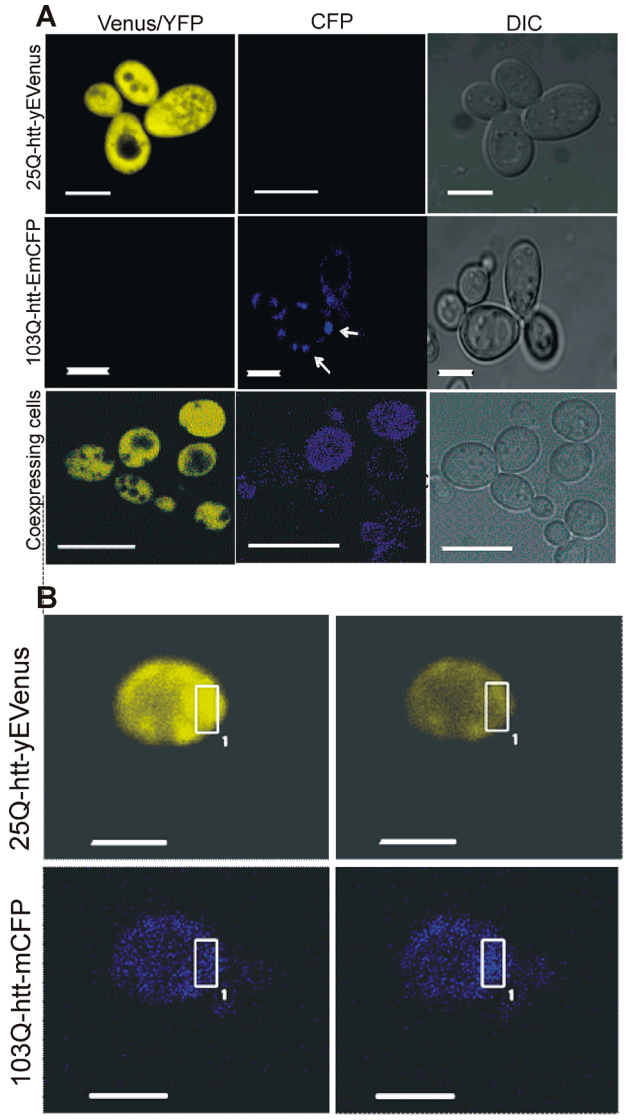

Figure 4. Expression of wild type and mutant huntingtin in yeast cells. (A) Confocal scanning laser microscopy of yeast cells expressing 25Q-htt-yEVenus and 103Q-htt-EmCFP alone and together was carried out. Arrows indicate presence of 103Q-htt-EmCFP aggregates. Fluorescence of yEVenus was monitored using excitation at 514 nm and emission at 515/30 nm, while 103Q-htt-EmCFP was scanned using excitation at 457 nm and emission at 450/35 nm. Bar = 10 μm. (B) FRET analysis. Fluorescence microscopy of cells coexpressing 25Q-htt-yEVenus and 103Q-htt-EmCFP recorded before and after photobleaching of 25Q-htt-yEVenus. Region of interest is shown by a white square. Bar = 10 μm. Images for a single cell are shown.

Gene Expression Analysis. Aggregation of mutant huntingtin has deleterious effects on the redox potential of the cell, elevating stress levels, compromising the cellular protein degradation mechanism, and resulting in loss of cell viability. Hence, we decided to monitor the expression levels of the genes involved in some of these pathways.

dx.doi.org/10.1021/cn400171d | *ACS Chem. Neurosci.* 2014, 5, 205−215

Table 1. Gene Expression Analysis in Cells Coexpressing 25Q-htt-EGFP and 103Q-htt-mRFP

	103Q-htt/25Q-htt		25Q-htt+103Q-htt coexpressed/103Q-htt	
target gene	fold change [$2^{-\Delta\Delta Ct}$]	*p*-value	fold change [$2^{-\Delta\Delta Ct}$]	*p*-value
Sod1	4.02 ± 0.06	1.12×10^{-6}	−1.61 ± 0.05	0.001532
Sod2	3.11 ± 0.49	0.012136	−2.91 ± 0.06	0.000346
Trx1	1.56 ± 0.31	0.143552	−1.41 ± 0.04	0.001737
Ctt1	2.30 ± 0.37	0.025566	−3.16 ± 0.01	2.10×10^{-7}
Glr1	−1.02 ± 0.09	0.842987	1.62 ± 0.16	0.020100
Gtt1	3.22 ± 0.57	0.01744	2.40 ± 0.03	0.000026
Gtt2	−1.12 ± 0.21	0.634263	1.21 ± 0.12	0.144484
Gpx2	−1.42 ± 0.15	0.108468	2.23 ± 0.22	0.005071
Gpx3	2.17 ± 0.18	0.002888	−1.81 ± 0.07	0.002689
Aif1	−1.28 ± 0.22	0.379114	1.84 ± 0.38	0.091713
Fis1	2.67 ± 0.28	0.003748	−2.18 ± 0.04	0.000194
Yca1	1.61 ± 0.14	0.010695	1.33 ± 0.18	0.144340
Bir1	1.09 ± 0.18	0.629034	1.16 ± 0.04	0.019261
Nma111	−1.04 ± 0.10	0.696791	1.58 ± 0.21	0.052551
Atg5	1.06 ± 0.15	0.726901	2.57 ± 0.29	0.005876
Tor1	1.11 ± 0.18	0.598716	−1.70 ± 0.01	0.000004
Tor2	−1.03 ± 0.09	0.724584	−1.62 ± 0.04	0.000633
Hsf1	2.88 ± 0.38	0.007514	−2.78 ± 0.01	9.17×10^{-7}
Hsp104	−1.31 ± 0.09	0.052097	1.11 ± 0.29	0.718165
Hsc82	1.89 ± 0.42	0.100194	−1.98 ± 0.04	0.000379
Ssa1	−2.23 ± 0.17	0.032339	−2.40 ± 0.07	0.000933
Ssa2	2.20 ± 0.23	0.005710	−2.69 ± 0.09	0.002378
Ssa3	15.38 ± 2.92	0.007875	−14.57 ± 0.02	5.74×10^{-07}
Sis1	−1.08 ± 0.22	0.728693	1.34 ± 0.38	0.420306
Ydj1	−2.14 ± 0.05	0.000671	−3.18 ± 0.06	0.000340

Most of the genes coding for antioxidant enzymes such as *Sod1*, *Sod2*, *Trx1*, *Ctt1*, *Glr1*, and *Gpx2* were found to be upregulated in cells expressing 103Q-htt alone, while their levels were lower in cells coexpressing 25Q-htt-EGFP and 103Q-htt-mRFP (Table 1). Expression of aggregated 103Q-htt-mRFP led to increased oxidative stress (Figure 3A), which may upregulate the mRNA pool of stress protective enzymes. Solubilization of the mutant protein lowered the oxidative stress (Figure 3A) and hence the transcriptome level of antioxidant enzymes. Interestingly, this difference in the transcriptome level was not replicated at the protein expression level. As an illustration, we carried out immunoblotting of the cell lysates with SOD1 antibody. Although the mRNA level of *SOD1* in cells expressing 103Q-htt-mRFP was about 4-fold higher than that in cells expressing 25Q-htt-EGFP (Table 1), presumably as a response of the cell to the higher oxidative stress challenge (Figure 3A), no significant difference in the expression levels of SOD1 was seen in cells expressing 25Q-htt-EGFP and 103Q-htt-mRFP, either alone or together (Figure 3D). Yeast cells treated with H_2O_2 exhibited upregulation of various antioxidant genes but the corresponding products were translationally downregulated.[23] Higher level of oxidative stress inhibits translation by increasing eIF2 phosphorylation.[24] This is especially true for the expression levels of antioxidant enzymes.[25] The overexpressed pool of mRNA is rapidly translated once the stress is lowered.

Aif1 (apoptosis inducing factor 1) (Ynr074 cP) is a mitochondrial protein which translocates to the nucleus during apoptosis.[26] Overexpression of *Aif1* has no effect on the viability of yeast cells. Even when *Aif1* is upregulated, exposure to stress conditions (e.g., H_2O_2) is necessary to trigger apoptosis. Aif1 has been reported to have oxidoreductase activity, which is important in maintaining the redox environment of the cell.[27] Recently, it has been shown that deletion of *Aif1* did not rescue cells from α-synuclein mediated toxicity in yeast cells.[28] This further suggests that Aif1 may not have a role in apoptosis in neurodegenerative diseases. The overexpression of *Aif1* in yeast cells coexpressing 25Q-htt-EGFP and 103Q-htt-mRFP (Table 1) may be related to its mitochondrial enzymatic function rather than its apoptotic function. No change in expression of *Aif1* was observed between cells expressing 103Q-htt-mRFP and 25Q-htt-EGFP (Table 1). In yeast cells, the mitochondrial fission protein Fis1 has a role in inhibition of apoptosis similar to Bcl proteins.[29] Upregulation of *Fis1* mRNA level indicates an increase in mitochondrial fission and has been observed in mammalian cells expressing mutant huntingtin and in brain samples from HD patients.[30] Abnormal mitochondrial fission is a hallmark of neurodegenerative diseases such as Huntington's disease, Parkinson's disease and Alzheimer's disease and is a characteristic feature of toxicity due to misfolding and aggregation of mutant huntingtin.[30] Significant upregulation of *Fis1* mRNA level in cells expressing 103Q-htt-mRFP was seen as compared to those expressing 25Q-htt-EGFP (Table 1). Expression of *Fis1* was downregulated in cells coexpressing 25Q-htt-EGFP and 103Q-htt-mRFP as compared to those expressing 103Q-htt-mRFP alone. Downregulation of *Fis1* and consequent restoration of normal level of mitochondrial fission may account for the improved viability of cells expressing 103Q-htt-mRFP in the soluble form in the presence of 25Q-htt-EGFP. Overexpression of Yca1 (yeast metacaspase), a cysteine protease, leads to apoptosis in cells.[31] It is associated with a number of chaperones such as Hsp104, Ssa1, Ssa2, Hsp42, and Ydj1. Based on its interaction with these chaperones, it has been proposed that Yca1 has aggregate-remodelling activity.[32] Upregulation of *Yca1* in cells expressing 103Q-htt-mRFP alone as compared to those expressing 25Q-

dx.doi.org/10.1021/cn400171d | ACS Chem. Neurosci. 2014, 5, 205−215

htt-EGFP (Table 1) indicated that increased aggregate-remodelling activity was a cellular defense mechanism in response to the formation of protein aggregates. No significant difference in expression of *Yca1* was seen in cells expressing aggregated 103Q-htt-mRFP when compared with cells coexpressing 25Q-htt-EGFP and 103Q-htt-mRFP (Table 1). Upregulation of *Yca1* gene indicates a concerted effort by the cell to clear toxic species due to the expression of 103Q-htt-mRFP. Some recent studies have also reported the role of Bir1 as an antiapoptotic factor.[33] Its overexpression protects cells from apoptosis, while its deletion increases apoptosis in yeast cells. No significant difference in expression of *Bir1* was seen in cells expressing 25Q-htt-EGFP as compared to cells expressing 103Q-htt-mRFP (Table 1). In cells expressing 103Q-htt-mRFP in the soluble form, marginal upregulation of this gene was observed, which can be construed as activation of protective mechanism leading to reduction in toxicity in these cells.

Nma111, a yeast homologue of mammalian HtrA2/Omi,[34] is a positive regulator of autophagy and helps in the degradation of damaged mitochondria as well as proteins involved in neurodegeneration such as mutant huntingtin and α-synuclein.[35] The expression level of *Nma111* was found to remain unchanged in cells expressing 103Q-htt-mRFP when compared with cells expressing the wild type protein (Table 1). Taken together with upregulation of *Fis1*, this indicates the failure of cells to protect mitochondria from damage and explains the increased toxicity observed in cells expressing the mutant protein alone. In cells expressing 103Q-htt-mRFP along with 25Q-htt-EGFP, a small but significant increase in expression of *Nma111* was observed (Table 1). Notably, overexpression of *Atg5* was also observed in cells expressing 103Q-htt-mRFP in the soluble form as compared to those expressing the protein in the aggregated form (Table 1). *Atg5* plays a central role in induction of autophagy and in the formation of autophagosomes along with Atg12.[36] Upregulation of autophagy is beneficial for clearance of mutant huntingtin from cells and reduction of cytotoxicity.[37] Upregulation of *Atg5* indicates that autophagy is promoted in coexpressing cells, matching with reduced cytotoxicity and enhanced viability observed in these cells. This also correlates well with the downregulation of *Tor1* and *Tor2* (Table 1), coding for negative regulators of autophagy, in these cells.[37] The upregulation of the entire autophagy mechanism in coexpressing cells further confirms its importance in maintaining cellular homeostasis. Upregulation of autophagy by Tor-dependent and -independent routes by a combination therapy of rapamycin and lithium (an inhibitor of inositol monophosphatase), respectively, has been shown to have beneficial effect in a Drosophila model of HD.[38] Thus, a fine balance between the positive and negative regulators of autophagy modulates the beneficial and adverse effects, respectively, of expression of mutant huntingtin.

Since protein misfolding activates the chaperone network of the cell, we decided to monitor the expression levels of genes coding for different cellular chaperones. Downregulation of the master regulator heat shock transcription factor, *Hsf1*, was observed in cells coexpressing 25Q-htt-EGFP and 103Q-htt-mRFP as compared cells expressing 103Q-htt-mRFP alone (Table 1). This was also reflected in the lower or unaltered expression of almost all the other genes studied in this class (Table 1). We cross-checked this by carrying out immunoblotting for Hsp104 to confirm if the mRNA levels are a true reflection of the levels of chaperone proteins in the cell. We indeed found no significant difference in the expression level of this hexameric chaperone in cells expressing 25Q-htt-EGFP and 103Q-htt-mRFP, either singly or together (Figure 3E). Molecular chaperones Hsp104, Ssa1, Ssa2, Ssa3, and Ydj1 have been shown to be essential for polyQ aggregation and toxicity.[39] In most of the yeast cells where the expression of these genes was knocked down, fluorescence (due to 103Q-htt-EGFP) was found to be diffused, with almost no visible aggregates. An extra copy of *Ydj1* in [PIN$^+$] strain resulted in increased toxicity due to 103Q-htt.[40] Increased solubilization of 103Q-htt-mRFP observed in coexpressing cells can thus be related to the downregulation of these genes. Previous studies with the Δ*Ssa1*/Δ*Ssa3* strain did not show any change in the aggregation and toxicity due to polyQ.[39] It was suggested that the results of the double deletion mutant cannot be used to extrapolate the effects of individual components since these could arise from induction of compensatory mechanisms.[40] The significantly high level of *Ssa3* (Table 1) observed with increased solubilization of the mutant protein requires cautious interpretation and has to be studied further. Inhibition of Hsp90 with the selective inhibitor NVP-AUY822 led to improved clearance of mutant huntingtin.[41] The effect of this inhibition was not due to activation of heat shock response. Thus, downregulation of the Hsp90 family chaperone Hsc82 in cells coexpressing 25Q-htt-EGFP and 103Q-htt-mRFP (Table 1) accounts for the improved viabilty of these cells as compared to those expressing 103Q-htt-mRFP alone.

Analysis of Relative Copy Number of 25Q-htt-EGFP and 103Q-htt-mRFP in Yeast Cells. Huntington's disease is an autosomal dominant disorder in which the presence of a single copy of the mutant allele can overcome the effect of the wild type allele. The transcriptional control of the wild type and mutant genes can play a crucial role in the progression of the disease. Solubilization of 103Q-htt-mRFP, in the presence of 25Q-htt-EGFP, was confirmed by native PAGE, immunoblotting and FRAP analysis. Decrease in cytotoxicity and enhancement of cell viability were also observed in these cells. Next, we measured the relative copy number of *25Q-htt-EGFP* and *103Q-htt-mRFP* in cells to understand if the level of the transcriptional product of each gene was important in deciding the phenotype.

Wild type and mutant *huntingtin* genes share a common sequence and differ only in the lengths of their polyglutamine repeats. The homopolymeric stretch is not amenable to high fidelity amplification due to slippage by the polymerase.[42] Hence, forward and reverse primers were designed which recognize the fluorophores tagged with huntingtin. Melting curve analysis confirmed that the primers were specific for the templates they recognize. No product was formed when *25Q-htt-EGFP* was amplified with primers specific for amplification of *mRFP* or when *103Q-htt-mRFP* was amplified with *EGFP*-specific primers (Figure S3, Supporting Information). Efficiency of amplification was confirmed by the appearance of a single, sharp peak in the melting curve. Relative C_t values were calculated by reverse transcription real time-PCR and normalized with the housekeeping gene *actin*. When expressed singly, the relative copy number of *25Q-htt-EGFP* (from pYES2-*25Q-htt-EGFP*) was 506.24 ± 83.51-fold higher ($p < 0.005$) than that of *103Q-htt-mRFP* (from pRS315-*103Q-htt-mRFP*). When coexpressed with 103Q-htt-mRFP (when the mutant protein was expressed in a soluble form), the relative copy number of *25Q-htt-EGFP* was 2.41 ± 0.30-fold lower ($p < 0.01$) than in cells expressing *25Q-htt-EGFP* alone. This

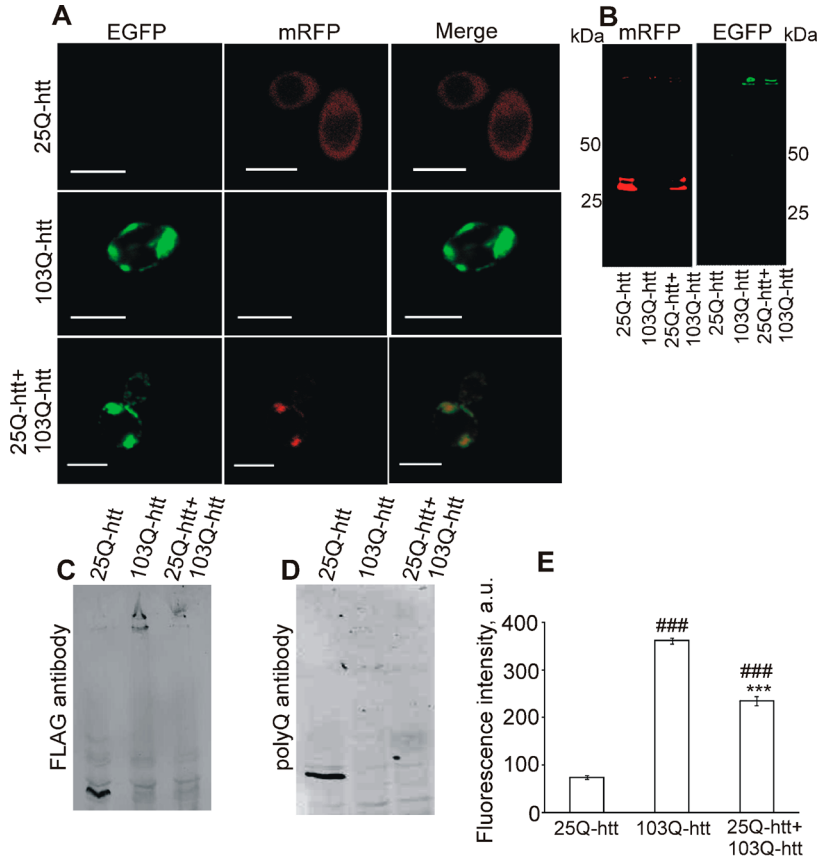

Figure 5. Sequestration of 25Q-htt by 103Q-htt. (A) Confocal microscopy of cells expressing 25Q-htt-mRFP (excitation at 547 nm and emission at LP 650 nm) and 103Q-htt-EGFP (excitation at 488 nm and emission at 510 nm) alone and together. Cells were visualized under 100× objective. Bar = 10 μm. (B) Native PAGE (12% cross-linked polyacrylamide gel) analysis of cell lysates expressing 25Q-htt-mRFP and 103Q-htt-EGFP. Gel was scanned in RFP and GFP modes on an image scanner (Typhoon Trio, GE Healthcare, Sweden). Molecular weight markers indicate positions of standard proteins on the same gel stained with Coomassie Blue. Aggregates of 103Q-htt-EGFP are clearly seen in the wells. For densitometric analysis, the intensity of the band for 25Q-htt-mRFP when expressed alone was assigned an arbitrary value of 1 and the corresponding band intensity of 25Q-htt-mRFP in coexpressing cells was calculated taking this as the base value. (C) Western blotting of cell lysates expressing 25Q-htt-mRFP and 103Q-htt-EGFP. The membrane was probed with mouse FLAG antibody (1:1000) as the primary antibody. (D) Western blotting of cell lysates expressing 25Q-htt-EGFP and 103Q-htt-mRFP. The membrane was probed with mouse polyQ antibody (1:5000) as the primary antibody. (E) Cytotoxicity was measured in cells expressing 103Q-htt alone and along with 25Q-htt by Sytox orange. Values shown are mean ± SEM of three independent experiments. $^{***}p < 0.001$ against cells expressing 103Q-htt alone; $^{###}p < 0.001$ against cells expressing 25Q-htt alone.

difference was, however, not discernible in the level of protein expression measured on the immunoblot (Figure 1C). Notably, the relative copy number of *103Q-htt-mRFP* in coexpressing cells was 4.32 ± 0.68-fold higher ($p < 0.01$) than in cells expressing *103Q-htt-mRFP* alone. This agrees well with the 2.7-fold increase in the expression level of 103Q-htt-mRFP observed in coexpressing cells on an immunoblot (Figure 1C). Thus, the presence of *25Q-htt-EGFP* affected the level of expression of *103Q-htt-mRFP* and vice versa. In cells coexpressing wild type and mutant proteins and where the mutant protein was expressed in the soluble form, the expression of *25Q-htt-EGFP* was still 50.61 ± 7.89-fold higher ($p < 0.01$) than that of *103Q-htt-mRFP*. The presence of *25Q-htt-EGFP* was beneficial for *103Q-htt-mRFP* as the expression of the latter was upregulated. On the other hand, the coexpression of the mutant allele was deleterious for the wild type allele as the relative copy number of the latter decreased. However, even under these conditions, the expression level of *25Q-htt-EGFP* was high enough to express 103Q-htt-mRFP in the soluble form. Next, we wanted to confirm if the observed solubility of the mutant protein was due to the high level of expression of the wild type protein.

Altering the Expression Levels of Wild Type and Mutant Huntingtin Alters the Solubility of the Proteins. The expression level of *25Q-htt* was reduced by cloning it into a low copy number plasmid (pRS315 vector), while *103Q-htt* was expressed from a high copy number, 2 μ plasmid (pYES2 vector). The wild type protein was expressed as a fusion protein with mRFP (25Q-htt-mRFP) while the mutant protein was tagged with EGFP (103Q-htt-EGFP). When expressed alone, 25Q-htt-mRFP was expressed in the soluble form while 103Q-htt-EGFP was present as aggregates (Figure 5A). In cells coexpressing 25Q-htt-mRFP and 103Q-htt-EGFP, the mutant protein was expressed in the aggregated form. Thus, when the wild type protein was expressed from a low copy number plasmid, it was unable to stabilize/solubilize the mutant protein against aggregation. More importantly, 25Q-htt-mRFP was found to be expressed as fluorescent puncta (Figure 5A). Aggregated 25Q-htt-mRFP was colocalized with 103Q-htt-EGFP, indicating sequestration of the wild type protein into the aggregated mutant protein. Reduction in solubility of 25Q-htt-mRFP was confirmed by native PAGE analysis (Figure 5B). Densitometric analysis showed that the fluorescence intensity of the band for the monomeric wild type protein was reduced

dx.doi.org/10.1021/cn400171d | ACS Chem. Neurosci. 2014, 5, 205−215

by 2.6-fold when coexpressed with 103Q-htt-EGFP. Immunoblotting with FLAG (Figure 5C) and polyQ (Figure 5D) antibodies also confirmed the decrease in solubility of the wild type protein.

The relative copy number of each gene was calculated in yeast cells. When each protein was expressed alone in cotransformed cells, the relative copy number of *103Q-htt-EGFP* was only 3.20 ± 0.41-fold higher ($p < 0.01$) than that of *25Q-htt-mRFP* even though the former was expressed from a high copy number plasmid (pYES2). This indicates that the toxicity of aggregated mutant huntingtin is high enough to affect the efficiency of transcription of the gene from the plasmid. Due to plasmid instability, only 0.1% of the cells have been reported to retain the plasmid expressing 103Q-htt after being grown on an induction plate for 3 days.[39] It was suggested that the toxicity effect of 103Q-htt aggregates is so harsh that loss the plasmid expressing the mutant protein gives a survival benefit to yeast cells even when they are grown on a selection plate. Comparison of expression of *25Q-htt-mRFP* in singly expressing cells showed 4.45 ± 1.06-fold ($p < 0.05$) higher expression than in coexpressing cells. This matches well with the 2.6-fold reduction of the wild type protein in coexpressing cells. When 25Q-htt-mRFP was coexpressed with 103Q-htt-EGFP, the relative copy number of *103Q-htt-EGFP* was 22.96 ± 3.26-fold higher ($p < 0.005$) than that of *25Q-htt-mRFP*, indicating reduction is cytotoxicity which allowed the plasmid to survive in the cell. This is despite both proteins being expressed in the aggregated form. Thus, the presence of 25Q-htt-mRFP is beneficial for the cell even when the wild type protein is present in the aggregated form.

Cell toxicity was further confirmed using Sytox dye.[21] When 103Q-htt-EGFP was expressed alone in the form of aggregates, the toxicity of yeast cells was higher as compared to the cells expressing 25Q-htt-mRFP alone (Figure 5E). When cells coexpressed 25Q-htt-mRFP and 103Q-htt-EGFP, the toxicity of the cells decreased significantly as compared to cells expressing 103Q-htt-EGFP alone. Thus, although both proteins were expressed in the aggregated form, the presence of the wild type protein lowered the toxicity due to the mutant protein.

Reports in the literature suggest that HD may occur as a result of gain of function of the toxic mutant protein or loss of function of the wild type protein.[10,16−18] Since the extent of aggregation is related to disease progression, any cellular condition that leads to reduction/inhibition of aggregation is likely to have a beneficial effect on cell survival. The work described here explains which mechanism (gain/loss) is likely to operate under which condition and how it modulates the phenotype of the affected cell. The relative expression level of the genes for wild type and mutant *huntingtin* decides the outcome. If the level of expression of the wild type protein is high, the toxic effect of the mutant protein is diminished. This explains the observed beneficial effect of wild type protein observed when it was cotransfected with mutant huntingtin at a mass ratio of 6:1 (full length wild type *huntingtin* to *exon1−72Q*).[17] When the expression level of the wild type protein is low, the toxic effect of the mutant protein predominates, so much so that the wild type protein is sequestered by aggregates of the mutant protein. This explains the formation of fibrillar structures by the wild type protein.[10] However, even under these conditions, the presence of the wild type huntingtin attenuates the toxic effect of the mutant protein. Another neurodegenerative protein, α-synuclein, has recently been shown to be involved in the assembly of SNARE-protein complexes at the presynaptic terminal.[43] The results presented here point to protein folding aid activity for wild type huntingtin protein, a function which appears to be dependent on its expression level in the cell.

METHODS

Materials. The yeast strain *Saccharomyces cerevisiae* BY4742 (MATα *his3Δ1 leu2Δ0 lys2Δ0 ura3Δ0*, [RNQ1$^+$]) was purchased from SAF Laboratories Pvt. Ltd., Mumbai, India. pRS315-*25Q-mRFP* and pRS315-*103Q-mRFP* were constructed by replacing *RNQ1* gene (in pRS315-*RNQ1-mRFP*) with the gene for *25Q-htt* or *103Q-htt* (from pYES2-*25Q-EGFP* or pYES2-*103Q-EGFP*, respectively) (Figure S1, Supporting Information). pKT90[44] and pKT212[44] were purchased from EUROSCARF (University of Frankfurt, Germany). pYES2-*25Q-htt-yEVenus* and pRS315-*103Q-htt-EmCFP* were constructed in the laboratory by replacing the gene for *EGFP* (in pYES2-*25Q-htt-EGFP*) with the gene for *yEVenus* (from pKT90) (Figure S2A, Supporting Information) and the gene for *mRFP* (in pRS315-*103Q-htt-mRFP*) with the gene for *EmCFP* (from pKT212) (Figure S2B, Supporting Information). Yeast nitrogen base (without amino acids) was purchased from HiMedia Laboratories Pvt. Ltd., Mumbai, India. Amino acids for amino acid dropout mixture were purchased from SRL Pvt. Ltd., Mumbai, India. Mouse anti-FLAG antibody and FITC-conjugated antimouse and antirabbit antibodies were purchased from Sigma-Aldrich, Bangalore, India. Mouse GAPDH antibody was a product of Abcam plc, Cambridge, U.K. Goat antimouse horseradish peroxidase (HRP)-conjugated monoclonal antibody and tetramethyl benzidine/hydrogen peroxide were obtained from Bangalore Genei, Bangalore, India. Dichlorodihydrofluorescein diacetate (DCFH-DA) was purchased from Cayman Chemical Company. Sytox orange was a product of Invitrogen. Oligo dT_{18} primer was purchased from Fermentas, Inc.. SYBR Premix Ex Taq (Perfect Real Time) kit was purchased from TaKaRa Bio, Inc., Japan. All other reagents and chemicals used were of analytical grade or higher.

Experimental Methods. *Expression of Wild Type and Mutant Huntingtin in Yeast Cells.* *Saccharomyces cerevisiae* BY4742 cells were cotransformed[45] with pYES2-*25Q-htt-EGFP* and pRS315-*103Q-htt-mRFP*, pRS315-*25Q-htt-mRFP* and pYES2-*103Q-htt-EGFP*, or pYES2-*25Q-htt-yEVenus* and pRS315-*103Q-htt-EmCFP* and were routinely grown in SC-LEU-URA media containing 2% dextrose/raffinose at 30 °C until A_{600} = 0.6−0.8. The expression of genes under the control of *GAL1* promoter (in pYES2) was carried out with 2% galactose for 10 h, while the expression of genes under the control of *CUP1* promoter (in pRS315) was induced with 500 μM $CuSO_4$ for 10 h at 30 °C. The expression of proteins was monitored using confocal microscopy, native PAGE, and immunoblotting. Images were aquired using an Eclipse E600 microscope (Nikon, Japan) and EZ-C1 v3.80 software. An objective lens (oil) of 100× (Plan Fluor) with 1.30 numerical aperture was used. Images were recorded using a digital camera DXM1200 (Nikon, Japan) and processed using ImageJ, a software available online.

Native PAGE Analysis and Immunoblotting. Yeast cells were lysed by the glass beads method.[46] After centrifugation, the samples were analyzed by native polyacrylamide gel (12% cross-linking) electrophoresis. The gel was scanned on an image scanner (Typhoon Trio, GE Healthcare, Sweden) in the fluorescence mode for detection of GFP or RFP signal. For immunoblotting, the proteins in cell lysates were separated by SDS denaturing polyacrylamide gel (12% cross-linking) electrophoresis. The protein bands were transferred to a nitrocellulose membrane (0.45 μm) and probed with FLAG, polyQ, SOD1, Hsp104, or GAPDH antibodies as the primary antibodies, as indicated. For detection of FLAG, polyQ, and GAPDH, anti-mouse FITC-conjugated or HRP-conjugated antibody was used as the secondary antibody. For detection of SOD1 and Hsp104, rabbit FITC-conjugated antibody was used as the secondary antibody. Densitometric analysis of bands was carried out using Image Quant (GE Healthcare, Sweden).

Measurement of Intracellular Oxidative Stress. The level of reactive oxygen species (ROS) was quantified using DCFH-DA.[47]

Induced cells were pelleted down and resuspended in 10 mM phosphate buffer, pH 7.4. Cells (1×10^7 each) were aliquoted into microcentrifuge tubes, and DCFH-DA (10 mM, in dimethylsulfoxide) was added at a final concentration of 10 μM followed by addition of H_2O_2 at a final concentration of 1 mM. The final reaction mixture was made up to 1 mL with phosphate buffered saline (10 mM, pH 7.4). The emission intensity of dichlorofluorescein (de-esterified and oxidized metabolite of dichlorodihydrofluorescein diacetate) was recorded after incubation for 1 h at an excitation wavelength of 504 nm and an emission wavelength of 519 nm. The emission spectrum of dichlorofluorescein was recorded in the absence of cells and was used as the control.

Yeast Cell Toxicity Assay. Induced cells were pelleted down, washed twice with 50 mM MES-NaOH buffer, pH 5.5, and resuspended in the same buffer. A_{600} was adjusted to 1.0. Sytox orange (50 μM, in dimethyl sulfoxide) was added to cell suspension (490 μL) to a final concentration of 1 μM.[21] The fluorescence emission of the dye was read at 570 nm, after exciting the samples at 547 nm.

Yeast Cell Viability Assay. Induced cells (9×10^3) were serially diluted 3-fold and plated on different selection plates. The plates were incubated at 30 °C, and growth of colonies was monitored for 2−3 days.

Fluorescence Recovery after Photobleaching (FRAP) Analysis. Fluorescence recovery after photobleaching (FRAP) is a technique in which fluorescent molecules present in a particular area are irreversibly photobleached by a high beam laser which is then allowed to recover at a low laser power. During recovery phase, the replacement of nonbleached molecules with bleached molecules is monitored using time lapsed imaging.[48] Soluble proteins tend to be more mobile than the aggregated species. Aggregates are generally localized in a particular area and little diffusion is seen around them. Thus, recovery after photobleaching in aggregates is less as compared to soluble species.

Induced yeast cells were pelleted down and washed with phosphate buffered saline, pH 7.4. Cells expressing 103Q-htt-mRFP alone or in the presence of 25Q-htt-EGFP were scanned under a confocal microscope. A region of interest (ROI) was selected in a single cell and FRAP was performed with 5 cycles of photobleaching with 100% laser power and 10 cycles of recovery at intervals of 60 s. The mobility fraction (R) was calculated using the formula, $R = (F_\infty - F_0)/(F_i - F_0)$, where F_∞ = fluorescence in the ROI after full recovery, F_i = fluorescence in the ROI prior to bleaching, and F_0 = fluorescence in the ROI just after photobleaching.[49]

Fluorescence Resonance Energy Transfer (FRET) Analysis. Fluorescence resonance energy transfer (FRET) has been used to study intermolecular interaction between proteins of interest tagged with GFP variants such as yEVenus (enhanced yellow fluorescent protein codon optimized for yeast system) and EmCFP (enhanced monomeric cyan fluorescent protein).[50] Acceptor photobleaching was employed to carry out the measurements.[44] In this method, the donor fluorescence is quenched if there is an energy transfer from donor to acceptor, so by photobleaching the fluorescence of the acceptor, increase in the fluorescence intensity of the donor is observed. Induced yeast cells were pelleted down and washed with phosphate buffered saline, pH 7.4. The acceptor fluorophore, 25Q-htt-yEVenus, was photobleached with 5% laser power and fluorescence intensity of 103Q-htt-EmCFP was measured before and after photobleaching. Under these conditions, the donor fluorophore was not bleached. The energy transfer efficiency, $FRET_{eff}$, was calculated as $(D_{post} - D_{pre})/D_{post}$, where D_{pre} and D_{post} are the fluorescence intensities of the donor prior to and following acceptor photobleaching, respectively. $FRET_{eff}$ is considered positive when $D_{post} > D_{pre}$.[22]

Gene Expression Analysis. Total RNA was isolated from yeast cells using the hot phenol method.[51] RNA obtained was reverse transcribed using oligo dT_{18} primer and MMLV reverse transcriptase according to the manufacturer's protocol. cDNA obtained was diluted (1:10) and used with SYBR Premix Ex Taq (Perfect Real Time) kit according to the manufacturer's protocol. Polymerase chain reaction was carried out using primers designed to amplify the desired genes (Table S1, Supporting Information).[52] Relative fold change in gene expression was calculated by comparative C_t method (also known as the $2^{-\Delta\Delta C_t}$ method).[53]

■ ASSOCIATED CONTENT

Ⓢ Supporting Information

Schematic diagrams for the construction of different vectors used in this work and details about primers used for RT-PCR experiments. This material is available free of charge via the Internet at http://pubs.acs.org.

■ AUTHOR INFORMATION

Corresponding Author

*Tel: 91-172-229 2061. Fax: 91-172-221 4692. E-mail: ipsita@niper.ac.in.

Funding

This work was supported by a research grant from Department of Science and Technology (Govt. of India) [Grant No. SR/SO/HS-101/2010]. A.A.S. is grateful to Council for Scientific and Industrial Research (CSIR) for the award of senior research fellowship. A.K.B. acknowledges the award of junior research fellowship by DST-INSPIRE programme.

Notes

The authors declare no competing financial interest.

■ ACKNOWLEDGMENTS

The authors are thankful to Prof. Michael Y. Sherman, Boston University School of Medicine, for the gifts of pYES2-*25Q-htt-EGFP* and pYES2-*103Q-htt-EGFP*. For construction of pRS315-*25Q-htt-mRFP* and pRS315-*103Q-htt-mRFP*, the original vector pRS315-*RNQ1-mRFP* was received from Prof. Douglas Cyr, University of North Carolina. The authors are grateful to Prof. Thomas O'Halloran, Department of Chemistry, Northwestern University, and Prof. John Glover, University of Toronto, Canada for the gifts of anti-SOD1 and anti-Hsp104 antibodies, respectively.

■ REFERENCES

(1) Ross, C. A., and Tabrizi, S. J. (2011) Huntington's disease: from molecular pathogenesis to clinical treatment. *Lancet Neurol. 10*, 83−98.

(2) Weiss, K. R., Kimura, Y., Lee, W. C., and Littleton, J. T. (2012) Huntingtin aggregation kinetics and their pathological role in a Drosophila Huntington's disease model. *Genetics 190*, 581−600.

(3) The Huntington's Disease Collaborative Research Group. (1993) A novel gene containing a trinucleotide repeat that is expanded and unstable on Huntington's disease chromosome. *Cell 72*, 971−983.

(4) Bates, G. (2003) Huntingtin aggregation and toxicity in Huntington's disease. *Lancet 361*, 1642−1644.

(5) Rigamonti, D., Bauer, J. H., De-Fraja, C., Conti, L., Sipione, S., Sciorati, C., Clementi, E., Hackam, A., Hayden, M. R., Li, Y., Cooper, J. K., Ross, C. A., Govoni, S., Vincenz, C., and Cattaneo, E. (2000) Wild-type huntingtin protects from apoptosis upstream of caspase-3. *J. Neurosci. 20*, 3705−3713.

(6) Gauthier, L. R., Charrin, B. C., Borrell-Pagès, M., Dompierre, J. P., Rangone, H., Cordelières, F. P., De Mey, J., MacDonald, M. E., Lessmann, V., Humbert, S., and Saudou, F. (2004) Huntingtin controls neurotrophic support and survival of neurons by enhancing BDNF vesicular transport along microtubules. *Cell 118*, 127−138.

(7) Zeitlin, S., Liu, J. P., Chapman, D. L., Papaioannou, V. E., and Efstratiadis, A. (1995) Increased apoptosis and early embryonic lethality in mice nullizygous for the Huntington's disease gene homologue. *Nat. Genet. 11*, 155−163.

(8) Wexler, N. S., Young, A. B., Tanzi, R. E., Travers, H., Starosta-Rubinstein, S., Penney, J. B., Snodgrass, S. R., Shoulson, I., Gomez, F., Ramos Arroyo, M. A., Penchaszadeh, G. K., Moreno, H., Gibbons, K.,

Faryniarz, A., Hobbs, W., Anderson, M. A., Bonilla, E., Conneally, P. M., and Gusella, J. F. (1987) Homozygotes for Huntington's disease. *Nature 326*, 194−197.
(9) Scherzinger, E., Sittler, A., Schweiger, K., Heiser, V., Lurz, R., Hasenbank, R., Bates, G. P., Lehrach, H., and Wanker, E. E. (1999) Self-assembly of polyglutamine-containing huntingtin fragments into amyloid-like fibrils: implications for Huntington's disease pathology. *Proc. Natl. Acad. Sci. U.S.A. 96*, 4604−4609.
(10) Busch, A., Engemann, S., Lurz, R., Okazawa, H., Lehrach, H., and Wanker, E. E. (2003) Mutant huntingtin promotes the fibrillogenesis of wild-type huntingtin: a potential mechanism for loss of huntingtin function in Huntington's disease. *J. Biol. Chem. 278*, 41452−41461.
(11) Steffan, J. S., Kazantsev, A., Spasic-Boskovic, O., Greenwald, M., Zhu, Y. Z., Gohler, H., Wanker, E. E., Bates, G. P., Housman, D. E., and Thompson, L. M. (2000) The Huntington's disease protein interacts with p53 and CREB-binding protein and represses transcription. *Proc. Natl. Acad. Sci. U.S.A. 97*, 6763−6768.
(12) Perutz, M. F., Johnson, T., Suzuki, M., and Finch, J. T. (1994) Glutamine repeats as polar zippers: their possible role in inherited neurodegenerative diseases. *Proc. Natl. Acad. Sci. U.S.A. 91*, 5355−5358.
(13) Snell, R. G., MacMillan, J. C., Cheadle, J. P., Fenton, I., Lazarou, L. P., Davies, P., MacDonald, M. E., Gusella, J. F., Harper, P. S., and Shaw, D. J. (1993) Relationship between trinucleotide repeat expansion and phenotypic variation in Huntington's disease. *Nat. Genet. 4*, 393−397.
(14) Nestor, C. E., and Monckton, D. G. (2011) Correlation of inter-locus polyglutamine toxicity with CAG•CTG triplet repeat expandability and flanking genomic DNA GC content. *PLoS One 6*, e28260.
(15) Djoussé, L., Knowlton, B., Hayden, M., Almqvist, E. W., Brinkman, R., Ross, C., Margolis, R., Rosenblatt, A., Durr, A., Dode, C., Morrison, P. J., Novelletto, A., Frontali, M., Trent, R. J., McCusker, E., Gómez-Tortosa, E., Mayo, D., Jones, R., Zanko, A., Nance, M., Abramson, R., Suchowersky, O., Paulsen, J., Harrison, M., Yang, Q., Cupples, L. A., Gusella, J. F., MacDonald, M. E., and Myers, R. H. (2003) Interaction of normal and expanded CAG repeat sizes influences age at onset of Huntington disease. *Am. J. Med. Genet., Part A 119A*, 279−282.
(16) Aziz, N. A., Jurgens, C. K., Landwehrmeyer, G. B., EHDN Registry Study Group, van Roon-Mom, W. M., van Ommen, G. J., Stijnen, T., and Roos, R. A. (2009) Normal and mutant HTT interact to affect clinical severity and progression in Huntington disease. *Neurology 73*, 1280−1285.
(17) Ho, L. W., Brown, R., Maxwell, M., Wyttenbach, A., and Rubinsztein, D. C. (2001) Wild type Huntingtin reduces the cellular toxicity of mutant Huntingtin in mammalian cell models of Huntington's disease. *J. Med. Genet. 38*, 450−452.
(18) Leavitt, B. R., Guttman, J. A., Hodgson, J. G., Kimel, G. H., Singaraja, R., Vogl, A. W., and Hayden, M. R. (2001) Wild-type huntingtin reduces the cellular toxicity of mutant huntingtin in vivo. *Am. J. Hum. Genet. 68*, 313−324.
(19) Mugat, B., Parmentier, M.−L., Bonneaud, N., Chan, H. Y. E., and Maschat, F. (2008) Protective role of Engrailed in a Drosophila model of Huntington's disease. *Hum. Mol. Genet. 17*, 3601−3616.
(20) Hands, S., Sajjad, M. U., Newton, M. J., and Wyttenbach, A. (2011) In vitro and in vivo aggregation of a fragment of huntingtin protein directly causes free radical production. *J. Biol. Chem. 286*, 44512−44520.
(21) Zakrzewska, A., Boorsma, A., Delneri, D., Brul, S., Oliver, S. G., and Klis, F. M. (2007) Cellular processes and pathways that protect *Saccharomyces cerevisiae* cells against the plasma membrane-perturbing compound chitosan. *Eukaryotic Cell 6*, 600−608.
(22) Llopis, J., Westin, S., Ricote, M., Wang, Z., Cho, C. Y., Kurokawa, R., Mullen, T. M., Rose, D. W., Rosenfeld, M. G., Tsien, R. Y., and Glass, C. K. (2000) Ligand-dependent interactions of coactivators steroid receptor coactivator-1 and peroxisome proliferator-activated receptor binding protein with nuclear hormone receptors can be imaged in live cells and are required for transcription. *Proc. Natl. Acad. Sci. U.S.A. 97*, 4363−4368.
(23) Shenton, D., Smirnova, J. B., Selley, J. N., Carroll, K., Hubbard, S. J., Pavitt, G. D., Ashe, M. P., and Grant, C. M. (2006) Global translational responses to oxidative stress impact upon multiple levels of protein synthesis. *J. Biol. Chem. 281*, 29011−29021.
(24) Vogel, C., Silva, G. M., and Marcotte, E. M. (2011) Protein expression regulation under oxidative stress. *Mol. Cell. Proteomics 10*, 1−12.
(25) Singh, K., Saleh, A. A., Bhadra, A. K., and Roy, I. (2013) Hsp104 as a key modulator of prion-mediated oxidative stress in *Saccharomyces cerevisiae*. *Biochem. J. 454*, 217−225.
(26) Wissing, S., Ludovico, P., Herker, E., Büttner, S., Engelhardt, S. M., Decker, T., Link, A., Proksch, A., Rodrigues, F., Corte-Real, M., Fröhlich, K. U., Manns, J., Candé, C., Sigrist, S. J., Kroemer, G., and Madeo, F. (2004) An AIF orthologue regulates apoptosis in yeast. *J. Cell Biol. 166*, 969−974.
(27) Miramar, M. D., Costantini, P., Ravagnan, L., Saraiva, L. M., Haouzi, D., Brothers, G., Penninger, J. M., Peleato, M. L., Kroemer, G., and Susin, S. A. (2001) NADH oxidase activity of mitochondrial apoptosis-inducing factor. *J. Biol. Chem. 276*, 16391−16398.
(28) Buttner, S., Bitto, A., Ring, J., Augsten, M., Zabrocki, P., Eisenberg, T., Jungwirth, H., Hutter, S., Carmona-Gutierrez, D., Kroemer, G., Winderickx, J., and Madeo, F. (2008) Functional mitochondria are required for alpha-synuclein toxicity in aging yeast. *J. Biol. Chem. 283*, 7554−7560.
(29) Fannjiang, Y., Cheng, W. C., Lee, S. J., Qi, B., Pevsner, J., McCaffery, J. M., Hill, R. B., Basañez, G., and Hardwick, J. M. (2004) Mitochondrial fission proteins regulate programmed cell death in yeast. *Genes Dev. 18*, 2785−2797.
(30) Shirendeb, U., Reddy, A. P., Manczak, M., Calkins, M. J., Mao, P., Tagle, D. A., and Reddy, P. H. (2011) Abnormal mitochondrial dynamics, mitochondrial loss and mutant huntingtin oligomers in Huntington's disease: implications for selective neuronal damage. *Hum. Mol. Genet. 20*, 1438−1455.
(31) Guaragnella, N., Bobba, A., Passarella, S., Marra, E., and Giannattasio, S. (2010) Yeast acetic acid-induced programmed cell death can occur without cytochrome c release which requires metacaspase YCA1. *FEBS Lett. 584*, 224−822.
(32) Lee, R. E., Brunette, S., Puente, L. G., and Megeney, L. A. (2010) Metacaspase Yca1 is required for clearance of insoluble protein aggregates. *Proc. Natl. Acad. Sci. U.S.A. 107*, 13348−13353.
(33) Shimogawa, M. M., Widlund, P. O., Riffle, M., Ess, M., and Davis, T. N. (2009) Bir1 is required for the tension checkpoint. *Mol. Biol. Cell 20*, 915−923.
(34) Padmanabhan, N., Fichtner, L., Dickmanns, A., Ficner, R., Schulz, J. B., and Braus, G. H. (2009) The yeast HtrA orthologue Ynm3 is a protease with chaperone activity that aids survival under heat stress. *Mol. Biol. Cell 20*, 68−77.
(35) Li, B., Hu, Q., Wang, H., Man, N., Ren, H., Wen, L., Nukina, N., Fei, E., and Wang, G. (2010) Omi/HtrA2 is a positive regulator of autophagy that facilitates the degradation of mutant proteins involved in neurodegenerative diseases. *Cell Death Differ. 17*, 1773−1784.
(36) Suzuki, K., Akioka, M., Kondo-Kakuta, C., Yamamoto, H., and Ohsumi, Y. (2013) Fine mapping of autophagy-related proteins during autophagosome formation in *Saccharomyces cerevisiae*. *J. Cell Sci. 126*, 2534−2544.
(37) Floto, A., Sarkar, S., Perlstein, E. O., Kampmann, B., Schreiber, S. L., and Rubinsztein, D. C. (2007) Small molecule enhancers of rapamycin-induced TOR inhibition promote autophagy, reduce toxicity in Huntington's disease models and enhance killing of mycobacteria by macrophages. *Autophagy 3*, 620−622.
(38) Sarkar, S., Krishna, G., Imarisio, S., Saiki, S., O'Kane, C. J., and Rubinsztein, D. C. (2008) A rational mechanism for combination treatment of Huntington's disease using lithium and rapamycin. *Hum. Mol. Genet. 17*, 170−178.
(39) Meriin, A. B., Zhang, X., He, X., Newnam, G. P., Chernoff, Y. O., and Sherman, M. Y. (2002) Huntington toxicity in yeast model

depends on polyglutamine aggregation mediated by a prion-like protein Rnq1. *J. Cell Biol. 157*, 997−1004.
(40) Gokhale, K. C., Newnam, G. P., Sherman, M. Y., and Chernoff, Y. O. (2005) Modulation of prion-dependent polyglutamine aggregation and toxicity by chaperone proteins in the yeast model. *J. Biol. Chem. 280*, 22809−22818.
(41) Baldo, B., Weiss, A., Parker, C. N., Bibel, M., Paganetti, P., and Kaupmann, K. (2012) A screen for enhancers of clearance identifies huntingtin as a heat shock protein 90 (Hsp90) client protein. *J. Biol. Chem. 287*, 1406−1414.
(42) Kovtun, I. V., and McMurray, C. T. (2008) Features of trinucleotide repeat instability in vivo. *Cell Res. 18*, 198−213.
(43) Burré, J., Sharma, M., Tsetsenis, T., Buchman, V., Etherton, M. R., and Südhof, T. C. (2010) Alpha-synuclein promotes SNARE-complex assembly in vivo and in vitro. *Science 329*, 1663−1667.
(44) Sheff, M. A., and Thorn, K. S. (2004) Optimized cassettes for fluorescent protein tagging in *Saccharomyces cerevisiae*. *Yeast 21*, 661−670.
(45) Gietz, D., St. Jean, A., Woods, R. A., and Schiestl, R. H. (1992) Improved method for high efficiency transformation of intact yeast cells. *Nucleic Acids Res. 20*, 1425.
(46) Einhauer, A., Schuster, M., Wasserbauer, E., and Jungbauer, A. (2002) Expression and purification of homogenous proteins in *Saccharomyces cerevisiae* based on ubiquitin-FLAG fusion. *Protein Expression Purif. 24*, 497−504.
(47) Wong, C. M., Zhou, Y., Ng, R. W., Kung, H. F., and Jin, D. Y. (2002) Cooperation of yeast peroxiredoxins Tsa1p and Tsa2p in the cellular defense against oxidative and nitrosative stress. *J. Biol. Chem. 277*, 5385−5394.
(48) Axelrod, D., Koppel, D. E., Schlessinger, J., Elson, E., and Webb, W. W. (1976) Mobility measurement by analysis of fluorescence photobleaching recovery kinetics. *Biophys. J. 16*, 1055−1069.
(49) White, J., and Stelzer, E. (1999) Photobleaching GFP reveals protein dynamics inside live cells. *Trends Cell Biol. 9*, 61−65.
(50) Piston, D. W., and Kremers, G. J. (2007) Fluorescent protein FRET: the good, the bad and the ugly. *Trends Biochem. Sci. 32*, 407−414.
(51) Collart, M. A., and Oliviero, S. (2001) Preparation of yeast RNA. *Curr. Protoc. Mol. Biol. 23*, 13.12.1−13.12.5.
(52) Rozen, S., and Skaletsky, H. (2000) Primer3 on the WWW for general users and for biologist programmers. *Methods Mol. Biol. 132*, 365−386.
(53) Schmittgen, T. D., and Livak, K. J. (2008) Analyzing real-time PCR data by the comparative CT method. *Nat. Protoc. 3*, 1101−1108.